3-1-1984

Space charge limit instabilities in electron beams

Evangelos A. Coutsias

D.J. Sullivan

Recommended Citation

Physical Review A, 27(3): 1535-1543

Space-charge-limit instabilities in electron beams

E. A. Coutsias and D. J. Sullivan*
Department of Mathematics, University of New Mexico, Albuquerque, New Mexico 87131
(Received 22 April 1982)

The method of characteristics and multiple-scaling perturbation techniques are used to study the space-charge instability of electron beams. It is found that the stable oscillating state (virtual cathode) created when the space-charge limit is exceeded is similar to a collisionless shock wave. The oscillatory solution originates at the bifurcation point of two unstable steady states. Complementary behavior (virtual anode) results when an ion beam exceeds its space-charge limit. The virtual cathode can also exist in the presence of a neutralizing heavy-ion background. The Pierce instability, where the electron and ion charge densities are equal, is a special case of this broader class. Estimates of the nonlinear growth rate of the instability at the space-charge limit are given.

I. INTRODUCTION

Since the discovery of the Child-Langmuir relation[1,2] it has been known that exceeding the limiting current of a diode leads to the development of a virtual cathode. Subsequently, numerous papers were written on experiments and theory relating to space-charge–limited flows. Reference 3 provides an excellent background and bibliography. More recently, the exact steady-state solutions for electron beams in one-dimensional relativistic diodes[4] and bounded drift spaces[5] were derived. It is easily seen that for sufficiently large currents there exist two steady states for an electron beam, only one of which is stable.[6] At the space-charge limit (SCL) these two states coalesce, and above the SCL they disappear.[7] As current is increased past the SCL, the beam develops a jump instability and relaxes into an oscillating state.

In the early 1960's, computer models were developed which quantitatively depicted the nonlinear oscillatory nature of the virtual cathode.[8–10] These were one-dimensional, nonrelativistic, electrostatic, multiple-sheet models. References 8 and 9 qualitatively pointed out many interesting dependencies of the oscillation frequency and potential minimum position on injected current, thermal spread, and circuit resistance. Reference 10 presents computer experiments with one and two species.

The phenomenon of virtual-cathode formation in intense relativistic electron beams figures prominently in a number of high-interest research areas. Devices used to produce high-current ion beams for inertial-confinement fusion—pinch reflex diodes[11,12] and reflex triodes[13,14]—depend on the virtual cathode to inhibit electron transport and use its potential well to accelerate ions. The recent concept of the spherical electron-to-ion converter[15] requires a virtual cathode.

The virtual cathode plays a dominant role in areas other than production of light-ion beams for fusion. It is attributed with the main role in collective ion acceleration in neutral gas.[16,17] Control of virtual-cathode motion is the mechanism for acceleration in the Ionization Front Accelerator.[18,19] It is also the acceleration method in two concepts for collective-effect accelerators.[20,21] A final application is the use of virtual-cathode oscillations to produce high-power short-wavelength microwaves.[22–25] Experiments using reflex triodes have already produced 1.4 GW of power with 12% beam-to-rf energy-conversion efficiency.[26]

In this paper we use multiple-scaling perturbation techniques to study the time-dependent behavior of a beam when the SCL is exceeded. We derive estimates for the nonlinear growth rate of the ensuing instability and show that even below the SCL the beam is unstable to sufficiently large perturbations. The method can be applied to a wide class of problems, but here we treat the short-circuited one-dimensional electrostatic diode depicted in Fig. 1 as the simplest model containing the appropriate physics. We show that, at least in one dimension, an arbitrary heavy-ion background does not alter the qualitative behavior of the beam and present numerical results that exhibit virtual-cathode oscillations for a neutral beam.

II. PHYSICAL DESCRIPTION

Simulations were carried out in conjunction with the theory presented in the next section using a two-dimensional, relativistic, electrostatic, particle-in-cell code. The code can solve self-consistently for the time-dependent trajectories of tens of thousands of plasma particles over thousands of plasma

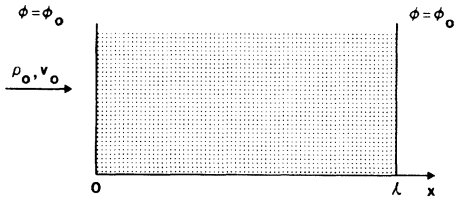

FIG. 1. Schematic of the short-circuited one-dimensional electrostatic diode modeled in this study.

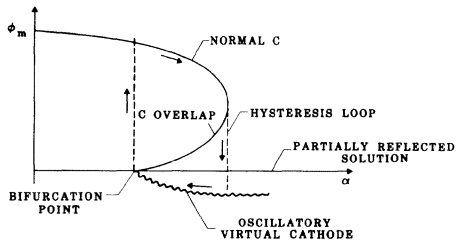

FIG. 2. Electrostatic potential minimum as a function of current α. Plot depicts the various possible solutions such as normal-C flow (stable), C-overlap (unstable), the partially reflected solution (unstable), and the oscillatory virtual cathode (stable). Motion around the hysteresis loop is denoted by arrows.

periods. All variables are expressed in dimensionless terms. Therefore length is in units of c/ω_p, time is measured in units of ω_p^{-1}, and particle velocity is given by

$$v_i=\beta_i\gamma \quad (i=1,2,3)\,,$$

where ω_p is the initial electron plasma frequency.

In these simulations a monoenergetic 51-keV electron beam is injected into a Cartesian geometry. The left and right boundaries are grounded, representing a planar short-circuited diode. Periodic boundary conditions in the transverse direction make configuration space effectively one-dimensional. In general, the simulation had 62 cells in the longitudinal direction modeling a length of $1.0c/\omega_p$. The time step was $0.0125\omega_p^{-1}$. Twenty particles were injected per cell.

A detailed discussion of the physical dynamics of the virtual cathode based on these numerical results is appropriate here. The usual graph of potential minimum ϕ_m in the diode versus electron-beam current α is shown in Fig. 2. The parameter α will be discussed later. When α is increased above the space-charge limit, ϕ_m jumps from the stable normal-C branch to the oscillatory stable branch. The amplitude and position of ϕ_m while on the oscillatory branch describe a limit cycle, as expected for a relaxation oscillation which this represents. Typical limit cycles are depicted in Fig. 3. As α is increased further, ϕ_m, the oscillation frequency, and virtual-cathode position within the diode asymptotically approach limiting values. If α is decreased, the oscillation amplitude $\Delta\phi_m$ decreases, and the position of ϕ_m moves toward the diode center. The electron flow reverts to the equilibrium steady state when the perturbation due to the rate of change of diode current below the space-charge limit is sufficiently large. This normally occurs before the bifurcation point is reached. The entire process forms a hysteresis loop, which is depicted in Fig. 2.

The virtual cathode originates at the bifurcation point. This is the intersection of the oscillatory state with the C-overlap[7] and partially reflected solution branches.[5] The bifurcation point cannot be reached in the short-circuited diode. Of the three branches emanating from it, two (the steady ones) are physically unstable while the oscillatory branch is numerically unstable at this point. This results because the limit cycle at the bifurcation point is infinitesimally small, so that simulation codes lose resolution before it can be reached. Loss of resolution creates a small-amplitude high-frequency oscillation observed in this study and previously.[9] This result is numerical, not physical.

This problem can be overcome if we eliminate the hysteresis loop. Then the C-overlap branch disappears, and we can get to the bifurcation point along the stable normal-C branch. This can be accomplished in several ways. The most appropriate in this study is to have a retarding potential difference across the diode equal to the injected-electron kinetic energy. Then the C-overlap solution vanishes, and the bifurcation takes place at the space-charge limit $\alpha_{\rm SCL}$. The oscillation can be described as a small perturbation on the beam rather than the radical change that results in the short-circuited diode when $\alpha_{\rm SCL}$ is exceeded. This analysis indicates that the onset of virtual-cathode formation occurs when the electron velocity in the steady state vanishes at some point inside the diode. For the short-circuited diode, this occurs at the diode center; for the biased diode, it occurs at $x \lesssim l$. Because the oscillation is a small perturbation on the steady-state fields in the biased diode, it is readily seen that the virtual-cathode oscillation period at onset is the electron transit time from the injection plane to the position where the velocity vanishes.

Finally, consider the particle dynamics during the oscillation period for counterclockwise limit cycles ($\alpha \lesssim \alpha_{\rm SCL}$) as in Fig. 3(c). At the point where the virtual-cathode position is a minimum and the potential well is starting to move to the right, its amplitude is too small to stop the electrons. When its motion is to the left it opposes the electron beam

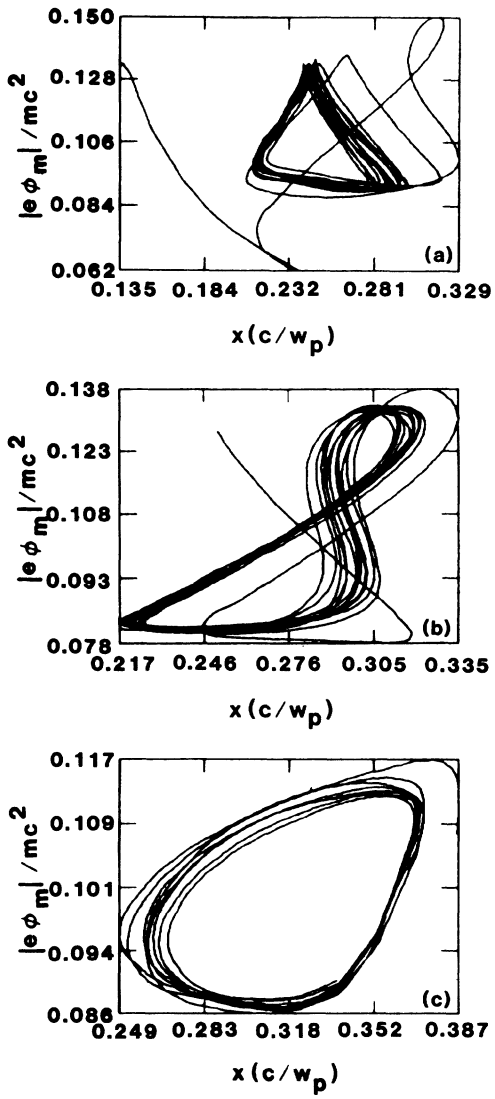

FIG. 3. Typical virtual-cathode limit cycles in the classical short-circuited one-dimensional diode with an injection energy of 51 keV. (a) $\alpha=2.5$, (b) $\alpha=2.0$, and (c) $\alpha=1.4$. Motion in (a) is clockwise and in (c) is counterclockwise. $l=1.0c/\omega_p$.

and causes particle bunching. Since the well is deeper, the stream velocity will vanish at some location and then become negative. Here, the second derivative of the velocity (d^2u/dx^2) is also negative. In this process the stream is continuously deformed to create a double-valued negative velocity protrusion. The entire system is three-valued (Fig. 4), as in a collisionless shock wave.[27] Here, the region of triple flow is not limited, as in usual collisionless shocks, by the presence of a transverse magnetic field,[28] but rather by the presence of the walls. Indeed, the reflected part detaches from the main beam and exits through the anode periodically, thus being responsible for the onset of oscillatory behavior in beam characteristics. As the potential minimum reaches the end of its left motion the two "lips" of the back reflected stream close. At this point no more electrons are reflected, and the well moves to the right, repeating the cycle.

For larger values of α the limit cycle is distorted into a figure "8" with one lobe having a clockwise motion and the other a counterclockwise one [Fig. 3(b)]. This transition continues until the motion is completely clockwise [Fig. 3(a)]. It indicates a change in the particle bunching process and is related to the fraction of current which is reflected versus transmitted from the injected-electron beam. In Fig. 3(a) most of the beam is reflected, whereas in Fig. 3(c) most electrons are transmitted.

III. THEORY

The one-dimensional motion of electrons in the diode is given by the equations of continuity and momentum conservation for the electrons plus Poisson's equation. They are expressed here as

$$\rho_{\tilde{t}}+(\rho v)_{\tilde{x}}=0 , \tag{1a}$$

$$v_{\tilde{t}}+vv_{\tilde{x}}=-(e/m)\xi , \tag{1b}$$

$$\epsilon_0\xi_{\tilde{x}}=\rho+\rho_h , \tag{1c}$$

where $0\le\tilde{x}\le l$. The subscripts denote differentiation with respect to that variable. Electron and heavy-ion charge densities, and electron velocity, electric field, time, and position, are indicated by ρ, ρ_h, v, ξ, $\tilde{t}$, and $\tilde{x}$, respectively. The appropriate boundary conditions are $v(0,\tilde{t})=v_0$, $\rho(0,\tilde{t})=\rho_0$, and $\int_0^l \xi\, d\tilde{x}=0$. An ion component is placed in Poisson's equation in order to discuss two-species space-charge flow. Conservation equations of mass and momentum for the heavy ions are not included, because it is assumed that their velocity does not change appreciably during their passage through the diode.

In order to simplify the mathematics, we introduce dimensionless equations for our model. They are

$$n_t+(nu)_x=0 , \tag{2a}$$

$$u_t+uu_x=-\alpha E , \tag{2b}$$

$$E_x=\alpha(n+I) , \tag{2c}$$

where $n=\rho/|\rho_0|$, $u=v/v_0$,

$$E=(e\epsilon_0/m\,|\rho_0|)^{1/2}\xi/v_0 ,$$

$$t=v_0\tilde{t}/l , \quad \tilde{x}=x/l ,$$

$$\alpha=(e\,|\rho_0|/\epsilon_0 m)^{1/2}l/v_0$$

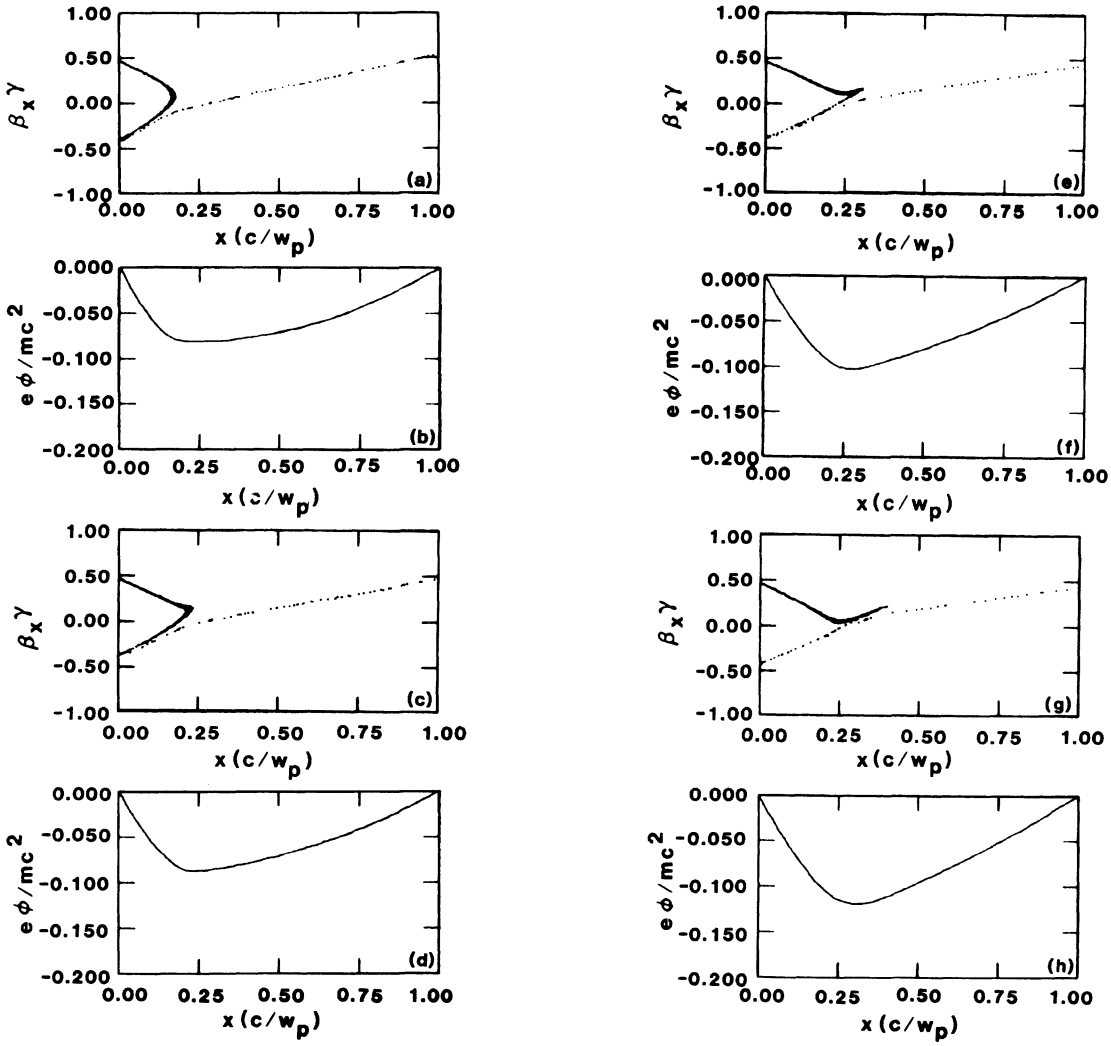

FIG. 4. Successive snapshots of electron-beam momentum space and corresponding potential shape in the diode for $\alpha=2.0$, $l=1.0c/\omega_p$. Time between frames is $0.5\omega_p^{-1}$. Initial beam kinetic energy is 51 kev.

(a dimensionless parameter related to current), and the ratio of heavy-ion to electron charge densities, $I=\rho_h/|\rho_0|$. Alternatively, α may be written as $l\omega_p/v_0$, where ω_p is the beam plasma frequency. The boundary conditions for electrons become $u(0,t)=1$, $n(0,t)=-1$, and $\int_0^1 E\,dx=0$. For an ion beam, $n(0,t)=1$; otherwise, the following derivation is the same.

A. Unneutralized beams

For an unneutralized beam, setting $I=0$ and solving by the method of characteristics[29,30] we find

$$n^{-1}=-\tfrac{1}{2}\alpha^2(t-s)^2+\alpha E_0(s)(t-s)-1\ , \qquad (3)$$

where s is the entry time for the particle occupying position x at time t, and $E_0(s)$ is the electric field at $x=0$. The particle trajectories are found by utilizing Eq. (2a), from which it follows that

$$\left[\frac{\partial x}{\partial s}\right]_t=n^{-1}\ . \qquad (4)$$

This yields

$$x=\tfrac{1}{6}\alpha^2(t-s)^3+\alpha\int_t^s E_0(s)(t-s)ds+(t-s)\ . \qquad (5)$$

Integration of the trajectory equation is hard for general time-dependent situations, because imposing the proper boundary conditions leads to a nonlinear integral equation for $E_0(t)$. However, several special cases can be solved exactly. The problem of injec-

tion into an empty diode can be integrated until the formation of a singularity in n, indicating the crossing of trajectories.[30] In this case, the stream velocity becomes three-valued, and one must use a Vlasov-equation description,[31] rather than system (2) that is derived assuming a single stream of monoenergetic particles. As described in Sec. II, this multistreaming is characteristic of the oscillatory state created when α exceeds its SCL value.

Using these equations we can derive a similar representation for Fig. 2 in terms of E_0 and α. For steady states, $E_0(t)=E_0$, a constant, we find

$$u=-n^{-1}=\tfrac{1}{2}\alpha^2(t-s)^2-\alpha E_0(t-s)+1\ , \quad (6a)$$

$$x=\tfrac{1}{6}\alpha^2(t-s)^3-\tfrac{1}{2}\alpha E_0(t-s)^2+(t-s)\ . \quad (6b)$$

Imposing the conditions $x=1$, $u=1$ at $t-s=t_0$, the particle transit time, we note that t_0 must satisfy

$$\tfrac{1}{12}\alpha^2 t_0^3-t_0+1=0\ . \quad (7)$$

This equation has two positive solutions for $0\le\alpha\le\frac{4}{3}$, coalescing at $\alpha=\frac{4}{3}$. The largest one, for $0\le\alpha<2\sqrt{2/3}$ does not correspond to a real flow. In Fig. 5 we show E_0 $(=\alpha t_0/2)$ vs α. This representation will be used in the discussion of nonlinear stability.

B. Neutralized beams

The Pierce instability occurs when electron and ion space-charge flow is considered in finite geometries where there is no potential difference across the boundaries.[32] The ions can be stationary or moving with respect to the electrons. Charge neutrality is maintained at the injection plane. This instability may have ramifications for charged-particle inertial confinement fusion because of its effect on neutralized-beam propagation in the reactor.[33] In this section, we show that the Pierce instability is a special case of electron and ion space-charge flow. In general, two-species flow has steady and oscillatory states analogous to one-species space-charge flow.

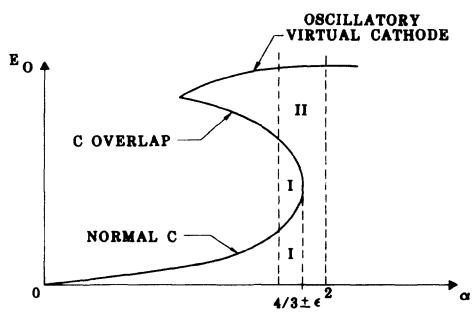

FIG. 5. Electric field at the injection plane vs current α for $I=0$. Plot depicts the normal C-flow (stable) and C-overlap (unstable) solutions. Oscillating virtual-cathode (stable) solution is also shown. Regions I and II define the domains of attraction of the normal-C and virtual-cathode solutions near the SCL, $\alpha=\frac{4}{3}$.

The steady-state behavior for the case of arbitrary I can be found in a manner similar to $I=0$. Rewriting system (2) in characteristic coordinates, we arrive at

$$\frac{d^2}{dt^2}\left[1+\frac{I}{n}\right]+\alpha^2 I\left[1+\frac{I}{n}\right]=0\ . \quad (8)$$

For positive ions $(I>0)$ the solution of (8) after satisfying the boundary conditions is

$$1+I/n=(1+I)\cos[\alpha\sqrt{I}\,(t-s)]+E_0\sqrt{I}\,\sin[\alpha\sqrt{I}\,(t-s)]\ . \quad (9)$$

Imposing conditions $x=1$, $u=1$ at $t-s=t_0$, we find the system

$$1=\frac{1}{I}t_0-\left[\frac{1-I}{\alpha I^{3/2}}\right]\sin(\alpha\sqrt{I}\,t_0)+\frac{E_0}{\alpha I}[\cos(\alpha\sqrt{I}\,t_0)-1]\ , \quad (10a)$$

$$1=\frac{1}{I}-\left[\frac{1-I}{I}\right]\cos(\alpha\sqrt{I}\,t_0)-\frac{E_0}{I}\sin(\alpha\sqrt{I}\,t_0)\ . \quad (10b)$$

For $I=1$, which implies charge neutralization, these equations reduce to the relations given in Ref. 34 for the Pierce instability. However, by varying I the curves shown in Fig. 6 are obtained. These are cuts at constant I through a three-dimensional contiguous surface. The space is defined by the axes $\tilde{E}=E_0 I^{1/2}$, $A=\alpha I^{3/2}$, and I. The surface is 2π periodic in A with the vertical plane at $A=2\pi$ being common for all values of I. For given A, a linearized analysis establishes that the equilibria denoted by the curves are stable (unstable) for the lowest (highest) value of $\tilde{E}$. At $I=1$, exchange of stability takes place at odd multiples of π. For $I<1$, exchange of stability occurs at the points where $dE_0/d\alpha\to\infty$.

It is evident from Fig. 6 that, for $I<1$, there are no stable equilibrium solutions in the neighborhood of $A=\pi$. Therefore one expects a virtual cathode to form when $I<1$ and A adiabatically increases to π. We have found, by using numerical simulation, that in this case the beam settles to an oscillatory state, similar to the virtual cathode for unneutralized

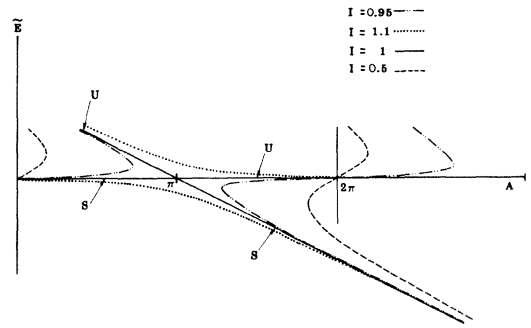

FIG. 6. Curves of scaled electric field at the injection plane $\tilde{E}$ vs scaled current A for various values of charge neutralization I. Curves represent slices through a three-dimensional surface. S and U indicate stable and unstable branches, respectively, for the $I=1$ slice.

beams.[31] By slowly increasing I past the neutral-beam value of 1 in our simulation, we have established that this oscillation persists. Indeed, finding this oscillatory state for $I>1$ by other means would have been difficult, because the simulation would tend to follow the stable steady-state branch that is present for all values of current.

C. Nonlinear stability analysis

For $I<1$, it is of interest to establish the properties of the beam instability at the SCL—generalized for $I\neq 0$ to mean the point where $d\alpha/dE_0=0$. We shall carry out the analysis for $I=0$, but our method can be applied to any similar jump phenomenon.

A linear stability analysis[6] about the steady state described by (7) results in the dispersion relation

$$(2+\beta)e^{-\beta}=2-\beta+\beta^3/(\alpha^2 t_0^3)\ , \tag{11}$$

where $\beta=i\omega t_0$. We have written the expression derived in Ref. 6 in terms of our dimensionless variables. For α near the SCL value we let

$$\alpha=\tfrac{4}{3}-\epsilon^2\ ,\quad \epsilon\ll 1 \tag{12}$$

and find from (7) that near this value, t_0 is approximately

$$t_0\simeq\frac{3}{2}\mp\epsilon\frac{3}{2\sqrt{2}}+O(\epsilon^2)\ , \tag{13}$$

where the $-$ $(+)$ sign corresponds to the lower (upper) branch in Fig. 5.

By substituting in (11), and assuming β small, we find that

$$i\omega=\beta\simeq\mp 2\sqrt{2}\epsilon+O(\epsilon^2)\ . \tag{14}$$

Since the linearized analysis led to time factors of the form $e^{i\omega t}$ in the perturbations, it follows that the lower branch in Fig. 5 is stable and the upper unstable, while at the SCL ($\epsilon=0$) we have neutral stability.

Above the value $\alpha=\frac{4}{3}$, linearized theory is not applicable. Utilizing multiple-scaling perturbation theory,[35] we can carry out a nonlinear stability analysis near $\alpha=\frac{4}{3}$. In system (2) we set $\alpha=\frac{4}{3}\pm\epsilon^2$. In this neighborhood, perturbations evolve on a "slow" time scale, depicted by $\tau=\epsilon t$.

Eliminating the electric field by combining (2b) and (2c) and utilizing τ, system (2) becomes

$$\epsilon n_\tau+(nu)_x=0\ , \tag{15a}$$

$$(\epsilon u_\tau+uu_x)_x=-(\tfrac{4}{3}\pm\epsilon^2)^2 n \tag{15b}$$

with conditions $u(0,\tau)=1$, $n(0,\tau)=-1$, and $\int_0^1 E\,dx=0$ rewritten as

$$\epsilon\int_0^1 u_\tau dx+\tfrac{1}{2}[u^2(1,\tau)-u^2(0,\tau)]=0\ . \tag{16}$$

Substituting the asymptotic expansions

$$u\sim\sum_{i=0}^{j}\epsilon^i u_i(x,\tau)+O(\epsilon^{j+1})\ ,$$

$$n\sim\sum_{i=0}^{j}\epsilon^i n_i(x,\tau)+O(\epsilon^{j+1})\ , \tag{17}$$

for u and n into (15) and equating coefficients of various powers of ϵ, there results a hierachy of equations for the u_i and n_i.

Solving the $O(1)$ system gives

$$(u_0-\tfrac{1}{2})(u_0+1)^2=2(2x-1)^2\ , \tag{18a}$$

$$n_0=-1/u_0\ . \tag{18b}$$

To solve the $O(\epsilon)$ system we introduce a new variable q by

$$x=\frac{16}{9}\left[\frac{q^3}{6}-\frac{3}{8}q^2\right]+q\ , \tag{19}$$

so that

$$u_0=\frac{16}{9}\left[\frac{q^2}{2}-\frac{3}{4}q\right]+1\ . \tag{20}$$

We then find

$$n_1=\frac{1}{u_0^2}u_1\ , \tag{21a}$$

$$u_1=C\frac{q(q-\frac{3}{2})}{u_0} \tag{21b}$$

with C a constant of integration which is, in general, a function of the slow time τ. To find $C=C(\tau)$ which determines the slow evolution of the perturbation $u_1(x,\tau)$ we need to go to the next order, $O(\epsilon^2)$. By substituting in the expressions for u_0,u_1,n_0,n_1 and eliminating n_2, we find that $u_2(x,\tau)$ satisfies

$$(u_0u_2)_{xx}+\frac{16}{9}\frac{1}{u_0^2}u_2=\frac{16}{9}\frac{C_\tau}{u_0}\int_0^q\frac{q(q-\frac{3}{2})}{u_0^2}dq+C^2\frac{q^2(q-\frac{3}{2})^2}{u_0^3}-C_\tau\left[\frac{q(q-\frac{3}{2})}{u_0}\right]_x\pm\frac{8}{3}\frac{1}{u_0}\,, \tag{22a}$$

$$u_2(0,\tau)=0\,,\quad u_2(1,\tau)=+\tfrac{9}{16}C_\tau\,. \tag{22b}$$

The solution to this inhomogeneous two-point boundary-value problem exists provided a certain orthogonality condition between the right-hand side and the solution of the adjoint problem that takes account of the boundary conditions is satisfied (Fredholm alternative theorem).[36] This leads to the desired equation determining $C(\tau)$,

$$aC_\tau+bC^2\pm c=0\,, \tag{23}$$

where a, b, and c are found to be

$$a=-\int_0^{3/2}\frac{q(q-\frac{3}{2})}{u_0^2}[\tfrac{16}{27}q^2(q-\tfrac{9}{4})+\tfrac{3}{2}]dq=1.6850\,, \tag{24a}$$

$$b=\tfrac{8}{3}\int_0^{3/2}\frac{q^3(q-\frac{3}{2})^3}{u_0^4}dq=-3.7968\,, \tag{24b}$$

$$c=\tfrac{8}{3}\int_0^{3/2}q(q-\tfrac{3}{2})dq=-1.5\,. \tag{24c}$$

In (23) the $(+)$ or $(-)$ signs indicate that we are above or below the SCL, respectively.

Above the SCL, we find

$$C(\tau)=-\frac{c}{b}\tan\left[\sqrt{cb}\left[\frac{\tau^+\tau_0}{a}\right]\right]\,; \tag{25}$$

and below the SCL,

$$C(\tau)=\begin{cases}\dfrac{c}{b}\tanh\left[\sqrt{cb}\left[\dfrac{\tau^+\tau_0}{a}\right]\right]\,, & |C(0)|<(c/b)^{1/2} \quad (26)\\[2ex] \dfrac{c}{b}\coth\left[\sqrt{cb}\left[\dfrac{\tau^+\tau_0}{a}\right]\right]\,, & |C(0)|>(c/b)^{1/2} \quad (27)\end{cases}$$

where τ_0 is a constant of integration. In general, small initial perturbations will lead to the solution

$$u(x,t)\sim u_0+\epsilon\sum_{i=1}^{j}C_i(\tau)e^{\omega_i t}u_i(x)+O(\epsilon^2)\,, \tag{28}$$

where ω_i are the various distinct solutions of the dispersion relation (11) at $\alpha=\frac{4}{3}$.[35,37] It is straightforward to show that all modes are such that $\mathrm{Re}\omega_i<0$ except one for which $\omega=0$. Thus all other modes will decay in the fast time scale and only the neutral mode ($\omega=0$) will persist. Our solution after a short time will look like

$$u\sim u_0+\epsilon C(\tau)\frac{q(q-\frac{3}{2})}{u_0}+O(\epsilon^2)\,. \tag{29}$$

From the given initial conditions it is easy to determine the initial condition for the neutral mode. Below the SCL, if the initial conditions are such that $C(0)>-(c/b)^{1/2}$, the solution will evolve to the stable lower branch in Fig. 5 (region I), while if $C(0)<-(c/b)^{1/2}$, $C\to\infty$ in finite time (Fig. 5, region II). Blowup in finite time also occurs above the SCL for any $C(0)$. This does not mean that the actual solution blows up, just that it evolves to a final state far away from the two steady-state branches shown in Fig. 5 and thus is not accessible by perturbation theory.

As can be seen in (25), the blowup above the SCL is described by a tangent function, therefore the growth rate we find for this case must be appropriately interpreted. Note that the linearized dispersion relation seems to suggest an imaginary exponential growth rate above the space-charge limit.[3,6] In view of our results, we see that this is actually misleading. Moreover, we find that even below the SCL the stable steady-state branch can be destabilized by sufficiently large perturbations.

Our results agree with the linear theory, provided we consider the limit where the latter becomes ap-

plicable. Thus we must compare the linear theory with (26) as $\tau \to +\infty$ (near the stable branch) and (27) as $\tau \to -\infty$ (near the unstable branch). To demonstrate this we set $\tau = \epsilon t$ in (26) and consider the limit $\tau \to +\infty$. Then

$$C(t) = \frac{c}{b}\tanh\left[\frac{\sqrt{cb}}{a}(\epsilon t + \tau_0)\right]$$

$$= \frac{c}{b}\frac{1-\exp\left[-\frac{2\sqrt{cb}}{a}(\epsilon t+\tau_0)\right]}{1+\exp\left[-\frac{2\sqrt{cb}}{a}(\epsilon t+\tau_0)\right]}$$

$$\simeq \frac{c}{b}\left[1-2\exp\left[-\frac{2\sqrt{cb}}{a}(\epsilon t+\tau_0)\right] + \cdots\right] . \quad (30)$$

We see that the decay rate of the perturbations as $t \to +\infty$ is equal to

$$\frac{2\sqrt{cb}}{a}\epsilon \approx 2.83\epsilon , \quad (31)$$

which is the same as that found by the linearized analysis.[6] This quantity is important as it also determines an initial "growth rate" for the jump instability above the SCL described by (25). If we substitute the original dimensional time variable into our expressions and write the deviation of α from its value at the SCL as

$$\epsilon = (\alpha - \alpha_{\rm SCL})^{1/2} = (\alpha - \tfrac{4}{3})^{1/2} , \quad (32)$$

we find that the "growth rate" is given by

$$D = (\alpha - \tfrac{4}{3})^{1/2}\frac{\sqrt{cb}}{a}\frac{v_0}{l} \quad (33)$$

or

$$D = \left[\frac{l\omega_p}{v_0} - \frac{4}{3}\right]^{1/2}\sqrt{2}\frac{v_0}{l} . \quad (34)$$

Of course, for the expansions in (28) to be valid, we must have $C(\tau) \ll 1/\epsilon$. However, while C is not too large, (25) gives a reliable estimate for the growth rate of the instability.

ACKNOWLEDGMENTS

This work was supported by Sandia National Laboratories. The authors are pleased to acknowledge many helpful discussions on virtual-cathode dynamics and the Pierce instability with R. B. Miller and B. B. Godfrey.

*Permanent address: Mission Research Corporation, 1720 Randolph Rd. S.E., Albuquerque, NM 87106.

[1]G. D. Child, Phys. Rev. (Ser. I) 32, 492 (1911).

[2]I. Langmuir, Phys. Rev. 21, 419 (1923).

[3]C. K. Birdsall and W. B. Bridges, *Electron Dynamics of Diode Regions* (Academic, New York, 1966), Chap. 3.

[4]H. R. Jory and A. W. Trivelpiece, J. Appl. Phys. 40, 3924 (1969).

[5]V. S. Voronin, Yu. T. Zozulya, and A. N. Lebedev, Zh. Tekh. Fiz. 42, 546 (1972) [Sov. Phys.—Tech. Phys. 17, 432 (1972)].

[6]R. J. Lomax, Proc. IEEE 108, 119 (1961).

[7]C. E. Fay, A. L. Samuel, and W. Shockley, Bell Syst. Tech. J. 17, 49 (1938).

[8]C. K. Birdsall and W. B. Bridges, J. Appl. Phys. 32, 2611 (1961).

[9]W. B. Bridges and C. K. Birdsall, J. Appl. Phys. 34, 2946 (1963).

[10]D. A. Dunn and I. T. Ho, AIAA J. 1, 2770 (1963).

[11]S. A. Goldstein and R. Lee, Bull. Am. Phys. Soc. 23, 763 (1978).

[12]R. A. Meyer, S. A. Goldstein, D. D. Hinshelwood, and G. Cooperstein, Bull. Am. Phys. Soc. 24, 977 (1979).

[13]D. S. Prono, J. M. Creedon, I. Smith, and N. Bergstrom, J. Appl. Phys. 46, 3310 (1975).

[14]D. S. Prono, J. W. Shearer, and R. J. Briggs, Phys. Rev. Lett. 37, 2 (1976).

[15]P. A. Miller, J. A. Halbleib, J. W. Poukey, and J. T. Verdeyen, J. Appl. Phys. 52, 593 (1981).

[16]J. W. Poukey and N. Rostoker, Plasma Phys. 13, 897 (1971).

[17]C. L. Olson, in *Collective Ion Acceleration-Springer Tracts in Modern Physics* (Springer, Berlin, 1979), Vol. 84.

[18]C. L. Olson, IEEE Trans. Nucl. Sci. NS-26, 4231 (1979).

[19]C. L. Olson, J. R. Woodworth, C. A. Frost, and R. A. Gerber, IEEE Trans. Nucl. Sci. NS-28, 3349 (1981).

[20]R. B. Miller, in *Proceedings of the Second International Topical Conference on High-Power Electron and Ion Beam Research and Technology* (Cornell University Press, Ithaca, N.Y., 1977), p. 613.

[21]R. B. Miller, in *Collective Methods of Acceleration*, edited by N. Rostoker and M. Reiser (Harwood, New York, 1979), p. 675.

[22]R. A. Mahaffey, P. Sprangle, J. Golden, and C. A. Kapetanakos, Phys. Rev. Lett. 39, 843 (1977).

[23]H. E. Brandt, A. Bromborsky, H. B. Bruns, and R. A.

Kehs, in Ref. 20, p. 649.

[24]J. M. Buzzi, H. J. Doucet, B. Etlicher, P. Haldenwang, A. Huetz, H. Lamain, C. Rouille, J. Cable, J. Delvaux, J. C. Jouys, and C. Peugnet, in Ref. 20, p. 663.

[25]D. J. Sullivan, in *Proceedings of the Third International Topical Conference on High-Power Electron and Ion Beam Research and Technology* (Institute of Nuclear Physics, Novosibirsk, USSR, 1979), p. 769.

[26]A. N. Didenko, G. P. Fomenko, I. Z. Gleizer, Ya. E. Krasik, G. V. Melnikov, S. F. Perelygin, Yu. G. Shtein, A. S. Sulakshin, V. I. Tsvetkov, and A. G. Zerlitsin, in Ref. 25, p. 683 (1979).

[27]R. Z. Sagdeev, *Reviews of Plasma Physics,* edited by M. A. Leontovich (Consultants Bureau, New York, 1966), Vol. 4, p. 23.

[28]S. S. Moiseev and R. Z. Sagdeev, Plasma Phys. 5, 43 (1963).

[29]G. B. Whitham, *Linear and Nonlinear Waves* (Wiley, New York, 1974).

[30]E. A. Coutsias and D. J. Sullivan (unpublished).

[31]D. J. Sullivan and E. A. Coutsias, in *High-Power Beams '81,* edited by H. J. Doucet and J. M. Buzzi (Ecole Polytechnique, Palaiseau, France, 1981), p. 371.

[32]J. R. Pierce, J. Appl. Phys. 15, 721 (1944).

[33]J. W. Poukey, J. P. Quintenz, and C. L. Olson, Appl. Phys. Lett. 38, 20 (1981).

[34]B. B. Godfrey, Mission Research Corporation Report No. AMRC-R-282, 1981 (unpublished).

[35]J. Kevorkian and J. D. Cole, *Perturbation Methods in Applied Mathematics* (Springer, Berlin, 1981).

[36]G. Birkhoff and G. Rota, *Ordinary Differential Equations* (Ginn, Boston, 1962).

[37]A. V. Paschenko and B. N. Rutkevich, Fiz. Plazmy 3, 774 (1977) [Sov. J. Plasma Phys. 3, 437 (1977)].